doi:10.1111/evo.13

Tempo and mode of mandibular shape and size evolution reveal mixed support for incumbency effects in two clades of island-endemic rodents (Muridae: Murinae)*

Dakota M. Rowsey,[1,2,3] Lawrence R. Heaney,[4] and Sharon A. Jansa[1,2]

[1]*Bell Museum of Natural History, University of Minnesota, St. Paul, Minnesota 55108*

[2]*Department of Ecology, Evolution, and Behavior, University of Minnesota, St. Paul, Minnesota 55108*

[3]*E-mail: rowse006@umn.edu*

[4]*Field Museum of Natural History, Chicago, Illinois 60605*

Received November 19, 2018

Accepted April 4, 2019

Existing radiations in a spatially limited system such as an oceanic island may limit the ecological opportunity experienced by later colonists, resulting in lower macroevolutionary rates for secondary radiations. Additionally, potential colonists may be competitively excluded by these incumbent (resident) species, unless they are biologically distinct (biotic filtering). The extant phenotypic diversity of secondary colonists may thus be impacted by lower rates of phenotypic evolution, exclusion from certain phenotypes, and transitions to new morphotypes to escape competition from incumbent lineages. We used geometric morphometric methods to test whether the rates and patterns of mandibular evolution of the Luzon "old endemic" rodent clades, Phloeomyini and Chrotomyini, are consistent with these predictions. Each clade occupied nearly completely separate shape space and partially separate size space. We detected limited support for decelerating and clade-specific evolutionary rates for both shape and size, with strong evidence for a shift in evolutionary mode within Chrotomyini. Our results suggest that decelerating phenotypic evolutionary rates are not a necessary result of incumbency interactions; rather, incumbency effects may be more likely to determine which clades can become established in the system. Nonincumbent clades that pass a biotic filter can potentially exhibit relatively unfettered evolution.

KEY WORDS: **Adaptive radiation, biotic filter, geometric morphometrics, macroevolution, interspecific competition, oceanic island.**

Adaptive radiation theory proposes that ecological opportunity, in which a lineage has access to an abundance of resources unused by competitors, can generate rapid evolutionary change to specialize on niches. The availability of unexploited niches promotes intraspecific variation necessary to accumulate new, ecologically distinct species (Parent and Crespi 2009) and may arise either from colonization of a depauperate ecosystem (Givnish et al. 2009) or from an evolutionary innovation that frees the lineage from existing competition to some degree (Wainwright et al. 2012). Over time, the radiation unfolds as intraspecific variation becomes partitioned into diverse species through disruptive selection in sympatry or adaptation in allopatry toward the resources on which they have specialized (Bolnick 2004; Tobias et al. 2014). From a quantitative standpoint, this theory suggests that release from competition is followed by an initially rapid occupation of available niches that declines over time as the opportunity for subsequent diversification decreases, resulting in a historical pattern of an initial burst of phenotypic evolution that decelerates toward the present (Mahler et al. 2010; Burbrink and Pyron 2010; Derryberry et al. 2011).

Despite developments in the ability to detect the historical signal of within-lineage adaptive radiation, the ecomorphological diversification of closely related lineages that colonize a system independently is insufficiently explored. Multiple colonizing

*This article corresponds to Roycroft, E. J. 2019. Digest: Colonizing rodents overcome ecological incumbency in an island system. Evolution. https://doi.org/10.1111/evo.13770.

lineages may serve to limit ecological opportunity because each group of colonists may compete with one another for available niches. If two colonization events by similar lineages are asynchronous, we should expect the lineage which arrived first to experience greater ecological opportunity than the secondary invader. Additionally, we might also expect the descendants of this initial colonist to competitively exclude potential invaders that are too ecologically similar (biotic filtering: Gillespie 2004; Emerson and Gillespie 2008). The advantage a primary colonizing lineage has over subsequently invading, ecologically similar lineages is known as an incumbency effect (Alroy 1996; Jablonski and Sepkoski 1996; Bambach et al. 2002). Incumbency effects can range in strength and scale from limiting colonization ability, to reducing abundance, to even facilitating colonization of subsequently colonizing lineages and as a result has highly variable effects depending on the system and spatiotemporal scale of interest (Almany 2004; Fukami 2004; Louette and De Meester 2007); nevertheless, the persistence of incumbency effects and the ability of subsequent clades to escape them requires further investigation.

Studies that have examined the macroevolutionary signature left by incumbency effects fall under two broad categories. First, several studies have examined clades that have escaped from incumbency effects, whether through a mass extinction event in the competing lineage (Webb 1985; Engel et al. 1998; Bambach et al. 2002) or dispersal to a competitor-deficient system (ecological release: Schluter 2000a). Importantly, studies following this approach often consider the focal clade in isolation, and rarely integrate the diversification history of this clade with respect to its close relatives. This lack of integration limits the ability to infer the history of competition prior to release from the effect. Second, researchers have inferred macroevolutionary dynamics from two potentially interacting radiations, but the scale of these studies is often too geographically broad, potentially limiting the ability to detect incumbency effects. In particular, previous studies have used this approach to examine the signature of incumbency effects at continental scales, usually recovering idiosyncratic patterns inconsistent with persistent interclade competition (Jønsson et al. 2015; but see Betancur-R. et al. 2012). For example, Schenk et al. (2013) and Alhajeri et al. (2016) used muroid rodents to test whether secondary colonists of continental systems experienced lower diversification rates and limited rates of ecological morphological evolution, respectively. These studies, in sum, recovered little support for decelerating rates of evolution in most systems, suggesting that the ecological opportunity model poorly explains the mode of evolution in Muroidea. However, studies such as these that focus on continental scales of macroevolution undoubtedly oversimplify the community structure and geologic history of the regions in question, especially for regions as biologically and geologically dynamic such as southeast Asia (Goldberg and Lande 2007; Ribas et al. 2007). Exploring these geographic regions at finer scales, with constituent clades that are more likely to compete with one another due to more recent phylogenetic divergence, may yield insights about macroevolutionary pattern and process that would otherwise be obscured. Lineages occupying oceanic archipelagic systems present ideal opportunities to test these hypotheses due to the potential for complex colonization history, spatial limitations, and striking adaptations arising from rapid evolution (Emerson 2002; Filardi and Moyle 2005; Schenk et al. 2013).

With this in mind, we chose to examine macroevolutionary incumbency effects at a fine spatial scale using two clades of "old endemic" murid rodents native to Luzon Island in the Philippines. Specifically, we examined evolution of mandibular morphology, because mandibular shape serves as a proxy for dietary niche, particularly with respect to differences associated with specialization on consuming invertebrates, seeds, or foliage (Grossnickle and Polly 2013; Maestri et al. 2016; Verde Arregoitia et al. 2017). Luzon is an oceanic island that began emerging as a continuously dryland area approximately 25 million years ago (Hall 2013). Since its formation, the island has been colonized an estimated six times by murine rodents, including the five colonization events identified by Jansa et al. (2006) and Rowsey et al. (2018): Phloeomyini, Chrotomyini, *Abditomys*, *Bullimus*, and *Rattus everetti*, and a potential sixth by *Crunomys fallax*. The first two invading lineages, Phloeomyini (*sensu* Lecompte et al. 2008) and Chrotomyini (considered by Lecompte et al. 2008 to be a member of Hydromyini and containing *Apomys*, *Archboldomys*, *Chrotomys*, *Rhynchomys*, and *Soricomys*; Rowsey et al. 2018), colonized between two and six million years (My) apart at approximately 12.8 and 8.4 million years ago, respectively (Rowsey et al. 2018). These two clades subsequently diversified to constitute nearly 90% of the rodent diversity on Luzon (Heaney et al. 2016a). Our previous analyses recovered no support for incumbency-influenced lineage diversification rates in these clades; however, rates of ecomorphological diversification for these lineages remain unexplored.

Prior field studies suggest that Phloeomyini and Chrotomyini greatly differ in dietary disparity: although the incumbent Phloeomyini range from generalist herbivores (i.e., eating some amount of fruits, seeds, and vegetative material), to bamboo foliage specialists, and to specialists on thick-coated seeds, most species within secondary-colonizing Chrotomyini vary mostly on a spectrum from omnivory to specializing on earthworms and soft-bodied arthropods (Heaney et al. 2016a,b). This apparent disparity in dietary variation begs several questions. First, is the partitioning of dietary variation the result of either depressed evolutionary rates or biotic filtering effects acting on Chrotomyini? Second, have incumbency effects acted on morphological evolution without a comparable signal in the lineages' diversification history? Finally, if interclade competition has influenced the morphological evolution of these two clades, is there evidence that

Chrotomyini has exhibited a rapid change in evolutionary process to escape the incumbency effects imposed by Phloeomyini?

To address these questions, we quantified mandibular shape and size for the constituent species of these two lineages. The analysis of mandibular variation in the phylogenetic framework established by Rowsey et al. (2018) allows us to test whether dietary evolution has occurred according to different processes for primary compared to secondary colonists. Specifically, we tested five predictions regarding how incumbency effects may have altered mandibular morphological evolution. First, we examined whether the two Luzon "old endemic" (LOE) clades occupied distinct areas of mandibular shape and size morphospace. We expect to observe this pattern if the ancestor for secondary-colonizing Chrotomyini could only establish itself on Luzon because it was distinct enough from the Phloeomyine lineages present on the island at the time, in other words, if Chrotomyini passed a biotic filter. Second, we tested whether either LOE clade evolved according to an "early burst" (EB) model of evolution, which predicts decreasing rates of morphological evolution over time (Harmon et al. 2010). Recovering decelerating evolution would suggest that morphological evolution is linked to the availability of ecological (specifically dietary) niches. Third, we tested whether morphological evolution in these two clades has exhibited discrete shifts to new "quantum zones" (Simpson 1953), as may be expected if Chrotomyini has evolved to escape incumbency effects imposed by Phloeomyini. Fourth, we tested whether extant morphological diversity in Chrotomyini resulted from greater convergent evolution than in Phloeomyini. If ecological incumbency plays a role in constraining chrotomyine morphospace occupancy, and by extension, niche evolution, we may expect to recover denser clustering of morphological variability, such that chrotomyines convergently resemble each other to a greater extent than phloeomyines do. Finally, we tested whether Chrotomyini exhibited lower rates of morphological evolution than Phloeomyini, assuming that no shifts in evolutionary rate occurred prior to colonization. We expected to recover this pattern if Chrotomyini had less ecological opportunity due to the diversification that had already occurred within Phloeomyini.

Materials and Methods

TAXON SAMPLING AND MORPHOMETRIC DATA SAMPLING

We photographed and landmarked a total of 337 mandibles representing 41 species, comprising all described LOE rodent species and two species undescribed at the time of writing. Specimens were sampled from the American Museum of Natural History (AMNH), the Field Museum of Natural History (FMNH), the Harvard University Museum of Comparative Zoology (MCZ), and the United States National Museum of Natural History (USNM). Only individuals with all molars completely erupted in both the cranium and mandible were chosen for study. The right ramus of the mandible was photographed on its buccal surface such that the anterior and posterior margins of the mandible (excluding the incisor) were coplanar. For specimens with mandibles damaged such that landmarks could not be taken, we used the left ramus if fewer landmarks would be lost and mirrored the image before data collection. The complete list of specimens sampled is presented in Table S1.

To account for intraspecific variation, we included multiple individuals from distinct geographic regions (e.g., different mountains and provinces) when available. When possible, we included two males and two females from each sampling locality, or four individuals if two of each sex were unavailable. Although they were included for our initial analyses of mandibular variation, we pruned *Batomys dentatus* and the single undescribed *Apomys* and *Rhynchomys* species from our comparative analyses of morphological evolution as no molecular phylogenetic data were available for these three species. Nearly all of our samples were obtained from rodents occurring on Luzon and minor outlying islands connected by shallow channels, although we included four individuals (out of 31 total) of *Chrotomys mindorensis* from Mindoro Island. We also excluded from our study old endemic species that are not found on Luzon, including five species of *Apomys* and the Greater Mindanao *Batomys* + *Crateromys* clade.

GEOMETRIC MORPHOMETRIC ANALYSIS AND MORPHOSPACE OCCUPANCY

All morphometric data were collected using the *geomorph* package in *R* (Adams and Otárola-Castillo 2013; R Core Team 2015). Twelve landmarks were collected from each mandible to quantify functional variation in mandibular morphology based in part on landmarks used in previous studies (Fig. 1, inset; Hautier et al. 2011; Grossnickle and Polly 2013). We estimated the positions of missing landmarks on applicable specimens using the thin-plate spline method implemented in the estimate.missing function of *geomorph* (Gunz et al. 2009), using the average configuration of completely represented conspecific mandibles as the reference to compute incomplete specimens. These landmark configurations were subjected to a generalized Procrustes analysis (GPA; Gower 1975, Rohlf and Slice 1990) to minimize differences among specimens due to scaling, translation, and rotation. These superimposed specimens were then analyzed using a principal component analysis (PCA) to determine variables that provided the greatest contribution to the variance of the dataset. In addition to shape data, we retained logarithmically transformed centroid size to analyze as a univariate trait to determine whether size and shape evolution displayed different signals of ecological opportunity or incumbency effects. Centroid size, or the square root of the summed distances from each landmark to the center of the landmark

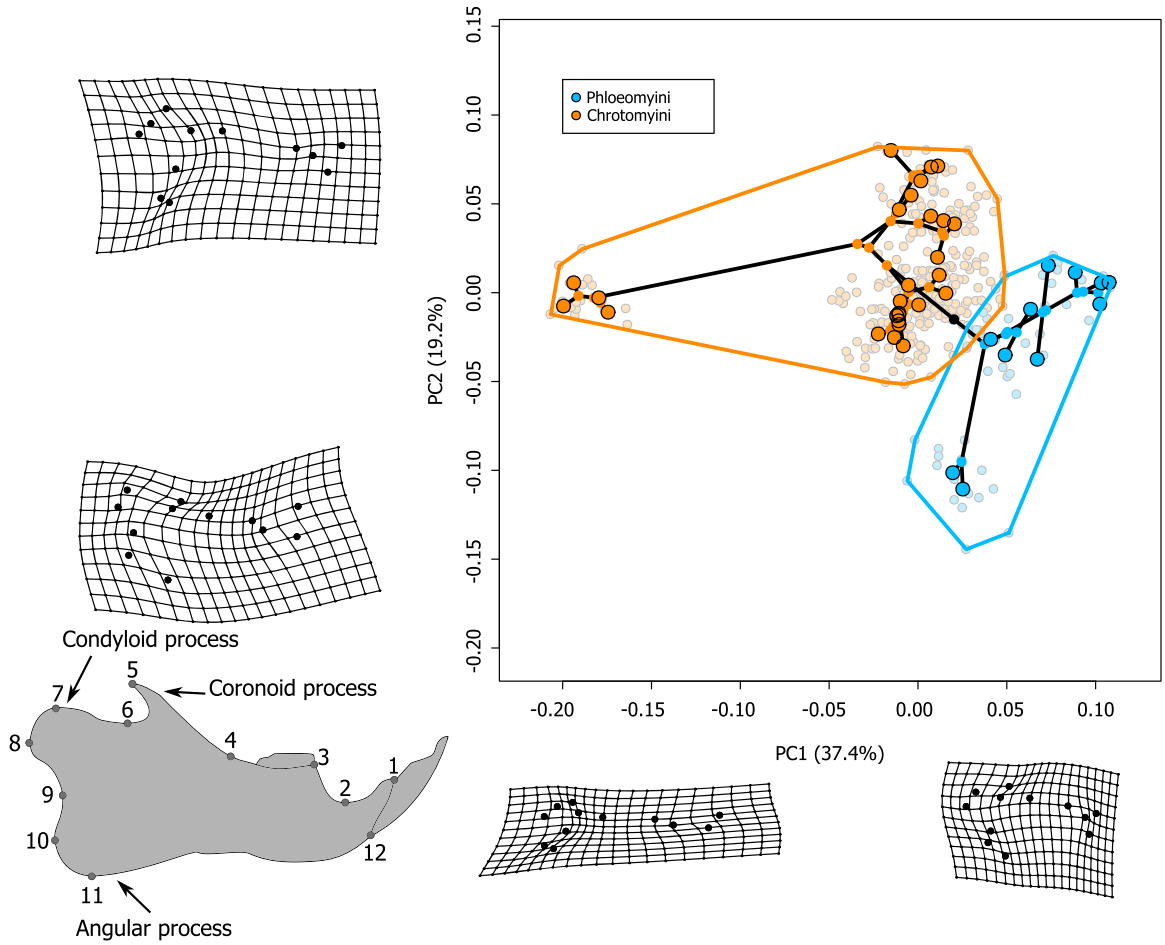

Figure 1. PC1 and PC2 of mandibular morphology for 41 Luzon old endemic rodent species ($n = 337$). Opaque enclosed circles represent species averages, with open circles the inferred ancestral state under Brownian motion evolution. Branches connecting points represent relationships among species according to pruned MCC tree from Rowsey et al. (2018; Figure 2). Transparent points represent individual specimens, the extremes of which are indicated with convex hulls for each clade. Thin-plate splines along axes show specimens with extreme scores and illustrate differences along these axes. Bottom-left: lateral view of a mandible indicating landmarks taken. Landmarks taken include (1) anterodorsal apex of incisive alveolus; (2) ventral nadir of diastema between incisor (I1) and first molar (M1); (3) anterior margin of M1 alveolus; (4) junction of coronoid process with body of mandible, defined by point at which a straight line following coronoid process first meets the body; (5) posterodorsal apex of coronoid process; (6) ventral nadir between coronoid and condyloid processes; (7) anterodorsal apex of condyloid process; (8) posterior apex of the condyloid process; (9) anterior nadir between condyloid and angular processes; (10) posterior apex of angular process; (11) ventral apex of angular process; and (12) anteroventral apex of incisive alveolus.

configuration, is a univariate measure used to rescale all specimens to a common size as a part of GPA. To ensure this was a reasonable proxy for body size, we regressed log-transformed centroid size against log-transformed head-and-body length.

Previous studies suggest that analysis of principal components can be misleading if phylogenetic relationships are unaccounted for (Revell 2009). However, we chose to present our results using standard PCA scores for three reasons. First, phylogenetic PCA requires specification of an underlying evolutionary model to compute the evolutionary variance–covariance matrix of the traits in question, and a primary goal of our study is inferring the evolutionary model responsible for generating the mandibular morphology of the focal clades. Second, whenever possible, we analyzed mandibular shape using approaches that determine multivariate distances among each species' GPA-transformed landmarks, which is equivalent to analyzing the entire component space generated under standard or phylogenetic PCA; this is because the phylogenetic rotation preserves Procrustes distances among specimens in multivariate space (Polly et al. 2013). Finally, when multivariate distance-based methods were unavailable for an analysis of interest, we used methods that can account for phylogenetic covariance among principal component axes whenever possible. Analyzing principal component axes using univariate comparative methods can incorrectly specify the model the data were generated under, regardless if phylogenetic transformations are performed (Uyeda et al. 2015). Due to the rapid proliferation

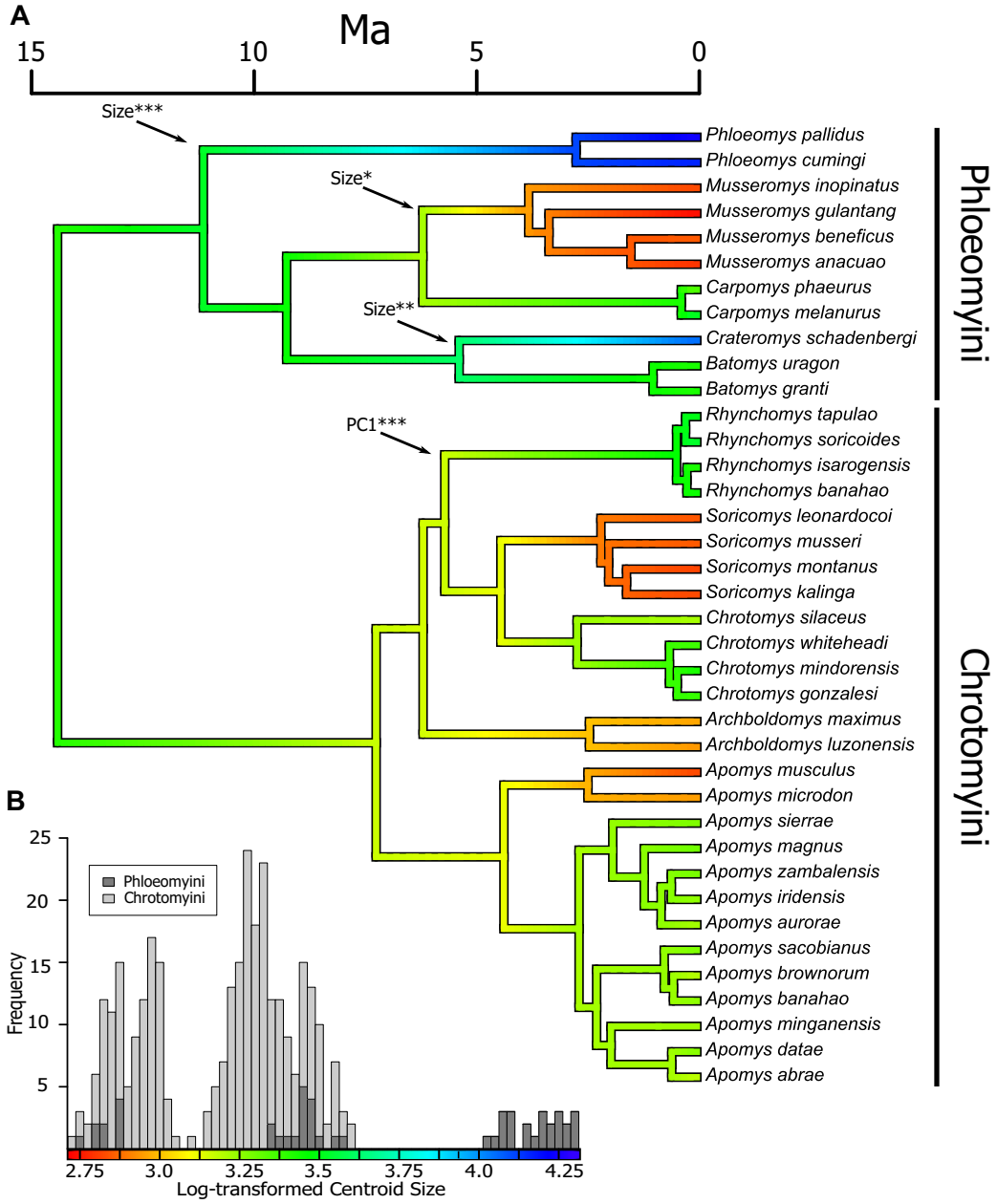

Figure 2. **(A) Phylogram illustrating relationships among Luzon old endemic rodents in relation to average log-transformed centroid size. Three additional species included in our phylomorphospace analysis (*Batomys dentatus*, *Apomys* sp., and *Rhynchomys* sp.) are not shown as no molecular data were available. Tree pruned from the Bayesian MCC tree inferred by Rowsey et al. (2018). Cooler colors indicate larger size and ancestral states were reconstructed based on maximum likelihood Brownian motion model parameters. Arrows indicate branches inferred to exhibit shifts in evolutionary mode and are labeled with the trait inferred to exhibit the shift. ***Posterior probability (PP) ≥ 0.95; **PP ≥ 0.9; *PP ≥ 0.85. (B) Histogram of log-transformed centroid size for the mandibular dataset (n = 337).**

of estimated parameters of multivariate analyses as more traits are examined and the relatively few species in Phloeomyini (11 species for which phylogenetic information was available), our rate-matrix-based multivariate analyses were limited to the first two principal component axes. The first two component axes for each clade-specific rotation account for 68.7% of chrotomyine shape variation and 58.9% of phloeomyine shape variation. We report results of our analyses generated under phylogenetic PCA in Tables S6–S8 and Figures S1-S2 and emphasize that they do not change our conclusions.

Using the *R* packages *ape* and *phytools* (Paradis et al. 2004; Revell 2012), we imported the maximum clade credibility (MCC) chronogram from Rowsey et al. (2018) to provide time-scaled evolutionary relationships with which we could conduct our comparative analyses. This tree was pruned to include only the focal taxa (i.e., the LOE rodents; Fig. 2). As the first step in our

morphometric analysis, we observed whether the patterns of morphological overlap in mandibular shape and size were consistent with biotic filtering, with areas of morphospace partitioned between clades, using phylomorphospace analysis of shape morphology (Klingenberg and Ekau 1996; Sidlauskas 2008) and a histogram of log-transformed centroid size to visualize the distribution of morphological variation. Recovering clade-specific morphospace partitioning would suggest that the assembly of the Luzon murine community is the result of interclade competitive factors and that the successful establishment of Chrotomyini may be the result of persistent ecological distinction between the two clades.

CLADE-SPECIFIC MODE OF MANDIBULAR EVOLUTION

To test whether the evolution of mandibular shape and size was consistent with decelerating ecological opportunity, we first partitioned the morphological data by LOE clade. For our analyses of shape evolution, we performed PCA on the GPA-transformed data for each clade. The first two PC axes for each clade were then fitted to a constant-rate Brownian motion model of evolution (BM; Felsenstein 1985) and a time-decelerating "early burst" model of trait evolution (Pagel 1999; Blomberg et al. 2003; Harmon et al. 2010) in a multivariate, maximum likelihood rate-matrix framework implemented in the *mvMORPH* package in *R* (Clavel et al. 2015; R Core Team 2015). These models were compared using a likelihood ratio test for each clade. It is important to note that, because we rotated each clade's mandibular shape separately, we did not compare the evolutionary rates between clades as a part of this analysis. For our analysis of size evolution, we performed a similar clade-specific model-fitting procedure using univariate BM and EB candidate models, likewise determining support using a likelihood ratio test for each clade. We additionally plotted multivariate shape and size disparity through time, measured in average pairwise Euclidean distances among species in subclades present at a given time in the tree, to visualize temporal changes in morphological evolution for each clade (Harmon et al. 2003). Average subclade disparity values near zero indicate each subclade accounts for relatively little disparity of the entire clade as a whole, meaning variation is clustered within subclades. Likewise, values near one indicate that each subclade accounts for a large proportion of the total disparity of the clade, meaning variation is dispersed among subclades.

In a complementary approach to this model-fitting test, we used a model adequacy approach to determine how well these best-fit models actually described trait evolution in each clade. This method, implemented in the R package *arbutus*, computes a series of metrics from the supplied data given an evolutionary model (Pennell et al. 2015). These metrics are compared to a distribution of simulated statistics to detect deviations from expected patterns given the model, for example, whether trait evolution is correlated with aspects of the tree topology or branch lengths. Deviations from the expected distributions suggest that the model inadequately describes aspects of trait evolution. As this approach has not been implemented in a multivariate framework, we calculated the model adequacy for each component axis and size separately using the *geiger* package in R (Harmon et al. 2008).

We additionally determined whether shape and size evolution in each clade exhibited evolutionary jumps along PC1, PC2, and centroid size. To do this, we compared the fit between a constant-rate BM process and a Lévy process that models rapid evolutionary jumps corresponding to a shift in evolutionary mode (Landis et al. 2013). We inferred model parameters and tested model fit using *Levolution* (Duchen et al. 2017). This program uses an expectation maximization (EM) approach to optimize model parameters given a range of jump strength (α) values from which to sample using a grid search procedure, followed by a Markov-Chain Monte Carlo (MCMC) estimation of rate shifts given the tree. This algorithm requires initial values for the Brownian motion model as well as initial parameters for the Poisson rate (λ) and jump strength (α) of jumps between parameter distributions. We specified initial BM parameters according to the maximum likelihood estimations for PC1, PC2, and centroid size evolution independently; initial Poisson rates (1 for PC1 and centroid size, 0.01 for PC2); and a distribution of 20 jump strength values ranging from 1 to 1000 for all traits, with an additional set of 20 strengths sampled ranging from 1 to 400 for PC2. For each α, the EM algorithm ran for a maximum of 100 iterations to optimize and was considered converged if two test statistics could not reject a model of no trend among parameter values (test statistic $T < 2$) and the parameter values exhibited approximately equal sign changes in slope between iterations (i.e., random fluctuations, test statistic $N > 0.5$). Parameter value sampling of the MCMC under both EM and the sampling of rate shift configurations on the tree were conducted with 10,000 samples, with samples retained after every 20 steps and the first 200 samples discarded as burn-in.

We also tested whether phloeomyine incumbency constrained the available morphospace for Chrotomyini to occupy, increasing convergence among species within that clade. To do so, we compared the clade-specific covariance of pairwise Euclidean distances among PC 1–5 and pairwise patristic distances from the MCC tree ($\mathrm{cov}(d,p) = x$). This covariance measures the extent to which sister species resemble each other more than nonsister species. A positive covariance suggests that sister species tend to resemble each other more so than nonsister species (prevalent phylogenetic signal), whereas a negative covariance suggests that nonsister species are more similar to one another than sister species (prevalent convergence). We compared the difference between clade-specific covariances ($x_P - x_C$) to 1000 results simulated under a clade-independent multivariate BM model

($x_{max} - x_{min}$). We interpreted support for increased convergent evolution among Chrotomyini as recovering an observed covariance ratio greater than 95% of the absolute values of simulated differences.

CLADE-SPECIFIC TEMPO OF MANDIBULAR EVOLUTION

In addition to examining patterns of diversification, we tested whether rates of mandibular shape and size evolution (σ^2) were diminished in Chrotomyini because of limited ecological opportunity, using two different approaches. In the first, we fit PC1–2 and log-transformed centroid size to candidate single-rate or multirate models of multivariate BM trait evolution in a rate-matrix-based likelihood framework. We tested four different partitioning schemes. The first two schemes constitute our null and alternative models testing whether evolution along these component axes is consistent with incumbency effects: (1) a single-rate BM model and (2) a two-rate model partitioned by clade. Additionally, we also sought to test whether the evolutionary rate for Chrotomyini is better modeled with a discrete process for *Rhynchomys*, which has a strikingly distinct morphology compared to the other LOE rodents, and thus included (3) a two-rate model partitioning the chrotomyine genus *Rhynchomys* versus the remaining LOE rodents. Finally, we tested whether the morphological evolution of these two clades is the result of both incumbency effects and evolutionary innovation of *Rhynchomys* and thus we included (4) a three-rate model partitioning Phloeomyini, *Rhynchomys*, and remaining Chrotomyini. The transitions between rate categories were generated using stochastic character mapping repeated 100 times for each model (Revell and Collar 2009). This approach calculates the position along a branch that confers the maximum likelihood of change in evolutionary rate along a branch in a phylogeny. This likelihood is computed using a priori designated rate categories and the evolutionary variance–covariance matrix of the PC and centroid size data (Revell and Collar 2009). We assigned equal prior probabilities for all root states and allowed rate category to change at any point along the respective branch. The model with the best placement of rate regimes was determined using the Akaike weight (w) calculated from the average of $n = 100$ AICc scores for each partitioning scheme (Akaike 1974; Hurvich and Tsai 1989).

Our second approach to assessing clade-specific evolutionary rates involved comparing evolutionary rates between groups in a distance-matrix-based framework (Adams 2014). This approach has the advantage of permitting analysis of trait matrices with high dimensionality relative to the number of taxa in each group. The evolutionary rate ratio of Phloeomyini to Chrotomyini ($\frac{\sigma^2_{mult(P)}}{\sigma^2_{mult(C)}}$) was computed from multivariate distances among species' GPA-transformed shape variables for each clade. This observed ratio was compared to those generated under a simulated distribution of rate ratios under a clade-independent BM process. This analysis was repeated for size evolution as it is still applicable under this distance-based framework. Recovering an observed ratio of evolutionary rates much greater than those generated under the simulated process would indicate that each clade evolved according to a different evolutionary process. In the context of clade-specific rates, we expect to recover a rate ratio favoring Phloeomyini if Chrotomyini experienced less ecological opportunity.

Results

MORPHOSPACE OCCUPANCY

Our principal component phylomorphospace analysis illustrates the mandibular shape diversity among Luzon murines (Fig. 1). Chrotomyini tend to exhibit slender mandibles with prominent, dorsally set coronoid and condyloid processes and thin, posteriorly projecting angular processes. By contrast, phloeomyines exhibit stout, compressed mandibles and prominent, shield-like angular processes with comparatively shorter and broader coronoid and condyloid processes. The PCA illustrates the high dimensionality of mandibular shape: the first eight component axes account for 90.2% of the variance in the dataset. PC1 primarily represents anterior–posterior telescoping versus compression of the mandible, whereas PC2 captures positioning and size of the coronoid/condyloid processes relative to the angular process (Fig. 1). These axes accounted for 37.4% and 19.2% of dataset variance, respectively. The morphospace occupancy of each clade along the first two PCs was almost entirely without overlap. This between-clade partitioning of morphospace illustrates the distinct mandibular morphology, presumably reflecting dietary disparity, of the two clades. PC3, which captured 10.0% of the dataset variation, primarily represents the inflection point of the anterior margin of the coronoid process (landmark 4), a landmark which exhibited substantial intraspecific variation. PC4 captured 7.7% of the dataset variation and represents the orientations of the fossae adjacent to the condyloid process. PC5 captured 5.6% of the dataset variation and primarily corresponds to relative compression versus expansion of the angular process, in other words, the distances between landmarks 10 and 11. Components 3–5 did not exhibit cladewise clustering (Table S2).

Log-transformed centroid size was highly correlated with log-transformed head and body length (adjusted R^2: 0.919). As such, we used log-transformed centroid size as a proxy for body size in subsequent analyses because these data were available for all specimens. Centroid size varied substantially within and between clades (Fig. 2), but particularly within Phloeomyini, which exhibited three distinct size categories: the small *Musseromys*, the mid-sized *Batomys* and *Carpomys*, and the large *Crateromys* and *Phloeomys*. In Chrotomyini, we found two size classes, the first comprising the small *Apomys* (subgenus *Apomys*), *Archboldomys*,

Table 1. Likelihood ratio tests (LRT) of decelerating morphological evolution fitted to PCs 1 and 2 of mandibular shape.

	Phloeomyini		Chrotomyini	
$\ln(L)_{BM}$[1]	44.07		133.4	
$\ln(L)_{EB}$[2]	44.07		136.5	
D[3]	0		6.211*	
df	1		1	
Parameter values	PC1	PC2	PC1	PC2
σ_0^2 (initial rate)	4.23×10^{-4}	1.92×10^{-4}	1.32×10^{-3}	1.13×10^{-3}
$\bar{\sigma}^2$(average rate)	4.23×10^{-4}	1.92×10^{-4}	7.12×10^{-4}	6.10×10^{-4}
θ (ancestral state)	3.64×10^{-3}	-2.79×10^{-3}	1.96×10^{-2}	1.60×10^{-2}
β (deceleration parameter)	N/A		–0.349	

Statistically significant result of LRT suggests a decelerating rate model of evolution better describes the rate of evolution in the given clade. An asterisk indicates the likelihood ratio D is statistically significant at $\alpha = 0.05$.

[1]Log-likelihood, Brownian motion model of evolution.

[2]Log-likelihood, early burst model of evolution.

[3]$D = 2 \times (\ln(L)_{EB} - \ln(L)_{BM})$.

and *Soricomys*, and the second including the mid-sized *Apomys* (subgenus *Megapomys*), *Chrotomys*, and *Rhynchomys* (Fig. 2).

CLADE-SPECIFIC MODE OF MANDIBULAR EVOLUTION

The goal of our first test of incumbency effects was to determine whether the rate of mandibular shape evolution decelerated over time, which would be consistent with the expectations of an adaptive radiation scenario. Mandibular shape evolution within Phloeomyini did not support a decelerating, EB model of evolution: the maximum likelihood estimate of phloeomyine evolution under EB evolution yielded a rate deceleration parameter $\beta = 0$, rendering it equivalent to a constant-rate model ($\ln(L)_{BM} = 44.07$, $\ln(L)_{EB} = 44.07$, $D = 0$, df $= 1$, $P \approx 1$; Table 1). By contrast, a model of decelerating evolutionary rate was supported for Chrotomyini ($\ln(L)_{BM} = 133.4$, $\ln(L)_{EB} = 136.5$, $D = 6.21$, df $= 1$, $P = 1.27 \times 10^{-2}$; Table 1). The average rate of evolution was higher in Chrotomyini than in Phloeomyini along both PC axes (Table 1). Our model adequacy results suggested these models fit each clade well, with the only poorly modeled aspects of trait variation occurring in PC1 evolution in Chrotomyini: with marginal significance, the EB model for this axis did not adequately account for among-branch rate heterogeneity ($C_{VAR} = 0.9672$, $P = 0.05395$) and trait-value-associated rate heterogeneity ($S_{ASR} = 6.129$, $P = 0.05195$; Table S3). Interestingly, we lost all support for an EB model of evolution when *Rhynchomys* was pruned from the dataset, instead inferring identical parameter estimates under our EB model to our BM model and a deceleration parameter $\beta = 0$. This suggests that our support for an EB model is driven entirely by the highly divergent morphology of *Rhynchomys*. The disparity-through-time (DTT) of multivariate shape corroborates this, illustrating a steep plummet in within-clade disparity at the time of splitting of *Rhynchomys* from the remaining

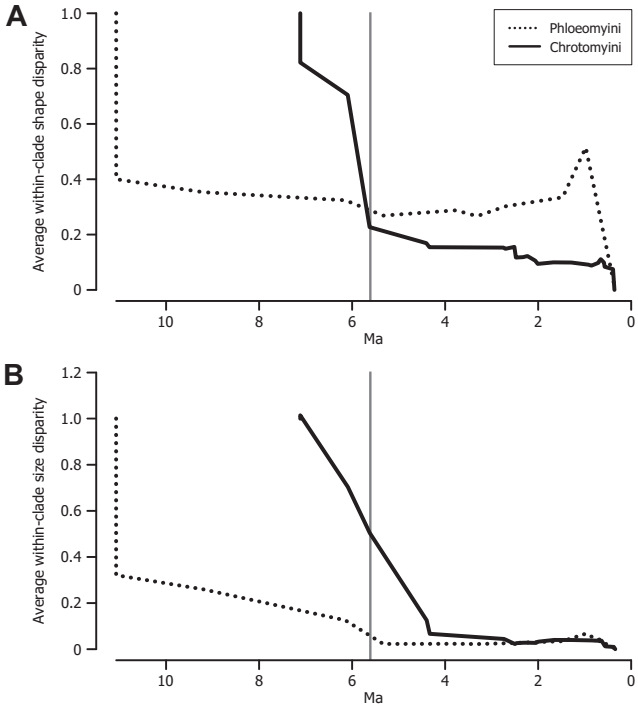

Figure 3. Disparity-through-time plots (Harmon et al. 2003) for multivariate mandibular shape (A) and logarithmically transformed centroid size (B). Within-clade disparity was measured as the ratio between the average pairwise Euclidean distances of each subclade node present at a given time in the clade's history and the average pairwise Euclidean distance among species in the entire clade.

chrotomyines, suggesting that at that point the average subclade does a poor job explaining the total amount of variation in the dataset (Fig. 3A). By contrast, Phloeomyini exhibits a strong decrease in average within-clade disparity at the first split within this clade, corresponding to the distinctiveness of *Phloeomys*. In

Table 2. Likelihood ratio tests (LRT) of decelerating morphological evolution fitted to log-transformed centroid size.

	Phloeomyini	Chrotomyini
$\ln(L)_{BM}$	−3.193	21.84
$\ln(L)_{EB}$	−2.959	24.35
D	0.4689	5.033*
df	1	1
σ_0^2 (initial rate)	2.13×10^{-2}	5.13×10^{-2}
$\bar{\sigma}^2$ (average rate)	2.13×10^{-2}	2.68×10^{-2}
θ (ancestral state)	3.64	3.12
β (deceleration parameter)	N/A	−0.437

Statistically significant result of LRT suggests a decelerating rate model of evolution better describes the rate of evolution in the given clade. An asterisk indicates the likelihood ratio D is statistically significant at $\alpha = 0.05$.

both clades, subsequent to the splits of these outlying lineages, remaining speciation events do little to contribute to within-clade disparity, except for a brief spike near the present in Phloeomyini, corresponding to the speciation of the morphologically similar species of *Batomys* followed by a decline corresponding to the recent split between morphologically distinct *Carpomys* species (Fig. 3A).

The clade-specific univariate analysis of log-transformed centroid size recovered a difference between clades in the best-fit model of size evolution, with Phloeomyini again favoring a constant-rate BM model and Chrotomyini favoring an EB model (Table 2). Both of these models were found to adequately describe the data, with no violations of model summary statistics. Unlike our results of shape evolutionary rate, our support for an EB model was robust to pruning *Rhynchomys* from the analysis ($\ln(L)_{BM} = 19.37$, $\ln(L)_{EB} = 21.61$, $D = 4.478$, df = 1, $P = 0.0344$). Interestingly, almost all size evolution occurred within the first three million years of the clade's existence on Luzon (Fig. 3B), roughly corresponding to genus-level divergence in the MCC tree generated by Rowsey et al. (2018). As with mandible shape, DTT of Phloeomyini size showed a large decrease in average within-clade disparity at the first split within this clade, corresponding to *Phloeomys*, and all subsequent splits failed to substantially contribute to within-clade disparity (Fig. 3B).

We recovered strong support for an evolutionary model that allowed shifts among evolutionary modes compared to a single-rate BM process for PC1, PC2, and centroid size (Table 3). With respect to mode-shift locations, we detected high posterior probability for a shift in evolutionary mode along PC1 on the branch of the phylogeny leading to *Rhynchomys* and evidence for three independent shifts in centroid size evolution in Phloeomyini with varying support (Fig. 2A). We did not recover strong support for shifts along any branch with respect to PC2 despite recovering strong support for this model.

Our final analysis comparing the mode of evolution between Chrotomyini and Phloeomyini tested whether Chrotomyini exhibited greater convergent evolution than did Phloeomyini resulting from limited morphospace availability. Although Phloeomyini exhibited a larger covariance of PC1–5 Euclidean distances and patristic distances than did Chrotomyini ($x_P = 0.179$, $x_C = 0.139$, $x_P - x_C = 4.05 \times 10^{-2}$), the difference between these covariances was statistically nonsignificant when compared to those simulated under a single-rate BM model (mean $x_{sim.max} - x_{sim.min} = 2.68 \times 10^{-1}$, $P = 0.90$; Fig. 4A). Similarly, convergence in size evolution did not exhibit a significant difference between clades ($x_P = 1.72$, $x_C = 3.06 \times 10^{-1}$, $x_P - x_C = 1.41$, $x_{sim.max} - x_{sim.min} = 1.29$, $P = 0.35$; Fig. 4B). Thus, we failed to support incumbency as forcing an increase in convergent evolution among Chrotomyini in either size or shape evolution.

CLADE-SPECIFIC TEMPO OF MANDIBULAR EVOLUTION

Our next series of analyses tested the hypothesis that the two clades differ from each other in their rate of mandibular evolution. Among the candidate models of single- versus multirate BM evolution, the best-fit model for the first two PCs was a two-rate model parameterizing *Rhynchomys* and the remainder of LOE rodent species under discrete rate categories, with moderate support (Table S4). Most simulated character histories gave strong support for this model over a single-rate model and a two-rate, clade-based model, but a three-rate model with Phloeomyini, *Rhynchomys*, and remaining Chrotomyini as discrete rate categories was supported as the best-fit model in 40% of simulations ($w = 0.37$). Our distance-based simulation approach, which allowed for multivariate comparisons of shape evolution using all the shape variation captured by our GPA, also revealed little support for clade-specific rates of morphological evolution. Although Phloeomyini exhibited a slightly higher average rate of shape evolution (Phloeomyini: $\sigma^2_{mult(P)} = 5.60 \times 10^{-5}$, Chrotomyini: $\sigma^2_{mult(C)} = 4.56 \times 10^{-5}$, $\frac{\sigma^2_{mult(P)}}{\sigma^2_{mult(C)}} = 1.23$), the observed ratio of multivariate evolutionary rates was not larger than expected under a single-rate model (mean $\frac{\sigma^2_{mult(max.sim)}}{\sigma^2_{mult(min.sim)}} = 1.17$, $P = 0.24$) (Figure 5A).

In contrast to shape evolution, size evolution was best explained by a two-rate, clade-specific model ($\ln(L) = 16.55$, $k = 3$, AICc = –26.41, $w = 0.68$; Table S5). This result is corroborated by recovering significantly higher rate of size evolution for Phloeomyini than expected under a single-rate process ($\sigma^2_{size(P)} = 2.20 \times 10^{-2}$, $\sigma^2_{size(C)} = 5.52 \times 10^{-3}$, $\frac{\sigma^2_{mult(P)}}{\sigma^2_{mult(C)}} = 3.98$, mean $\frac{\sigma^2_{size(max.sim)}}{\sigma^2_{size(min.sim)}} = 1.61$, $P = 0.01$) (Figure 5B). Recovering this significantly lower rate of size evolution within Chrotomyini is consistent with incumbency effects and represents

Table 3. Likelihood ratio tests (LRT) of BM versus Lévy evolution of mandibular shape (PC1 and PC2) and size.

	PC1	PC2	Centroid size
$\ln(L)_{BM}$	86.25	84.89	12.10
$\ln(L)_{L}$	106.6	95.45	28.90
D	40.76*	21.12*	33.61*
df	2	2	2
σ_0^2 (initial rate)	6.123×10^{-5}	9.851×10^{-5}	1.526×10^{-3}
θ (ancestral state)	3.062×10^{-2}	-4.215×10^{-2}	3.390
α (jump strength)	538.9	43.00	205.9
λ (jump rate)	1.009×10^{-2}	3.008×10^{-2}	9.218×10^{-2}

An asterisk indicates the likelihood ratio *D* is statistically significant at α = 0.05. Note that although we recovered strong support for a Lévy process along PC2, we did not recover high posterior probability for any evolutionary shifts on the tree.

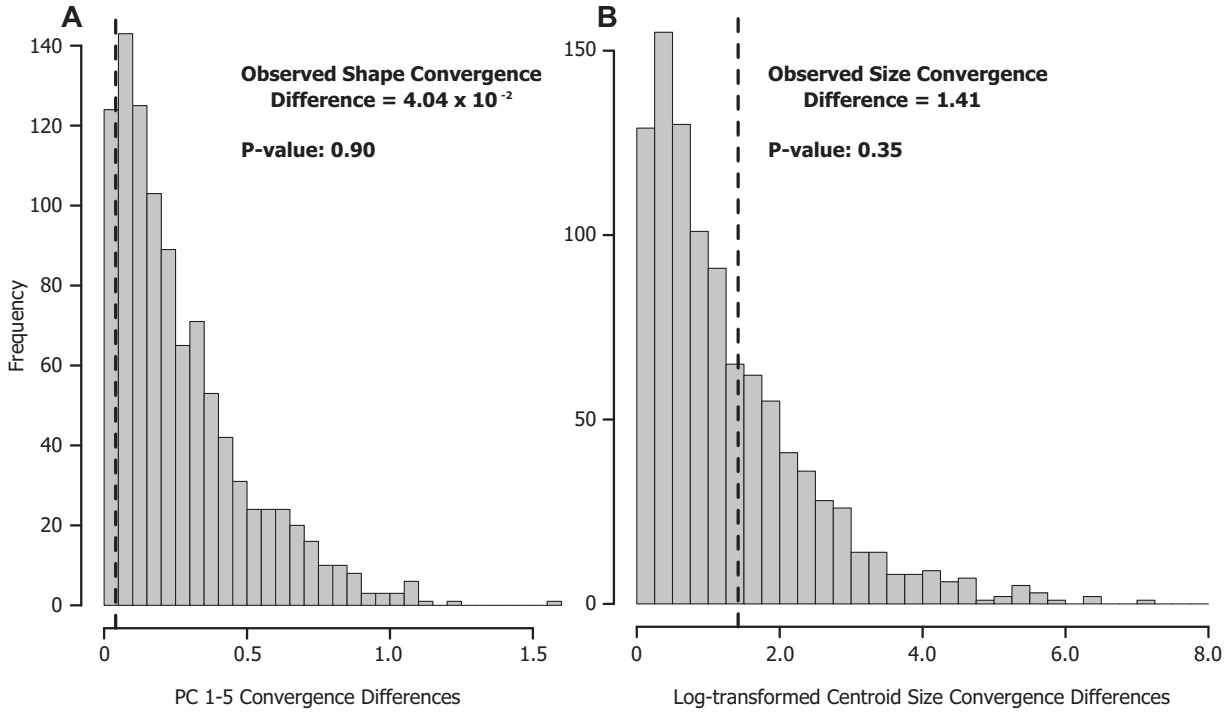

Figure 4. Histograms showing distribution of differences in cladewise covariances between Euclidean and patristic distances as a comparison of convergence between clades. (A) differences in PC 1–5 shape convergence are illustrated. (B) Differences in convergences based on Log-transformed centroid size are illustrated. The dashed line indicates the observed difference in covariances between Phloeomyini and Chrotomyini, and the gray bars represent differences simulated under a clade-independent Brownian motion process.

evidence of evolutionary rates consistent with this hypothesis among LOE murines.

Discussion

Our results suggest a complex relationship among incumbency effects, ecological opportunity, and morphological evolution (Table 4). Rather than inherently constraining the tempo or mode of evolution of secondary colonists, incumbency's strongest effects on morphological evolution appear to be establishing an initial biotic filter on subsequently colonizing lineages. This is best illustrated in our shape phylomorphospace analysis (Fig. 1), where the two clades exhibit almost no overlap, and the area each clade occupies is consistent with the ancestral chrotomyine lineage being already ecologically distinct with respect to diet from Phloeomyini extant at the time of chrotomyine colonization due to ancient divergence in allopatry (Tobias et al. 2014).

The morphospace occupancy of Chrotomyini is surprising in its diversity. In particular, *Rhynchomys* represents a rapid evolutionary innovation couched among species that are evolving disparate mandibular shapes at a constant, slower, rate (Fig. 2, Table S4). This rapid evolution in a secondary-colonizing clade illustrates that incumbency does not necessarily restrict the ability

Table 4. Summary of hypotheses and conclusions surrounding incumbency effects in the Luzon old endemic rodents.

	Conclusion		
Hypothesis	Lineage diversification	Mandibular shape evolution	Body/mandible size evolution
Secondary colonists occupy distinct areas of trait space from incumbent clades due to biotic filtering of ecologically similar species	Not applicable	Strongly supported. Each clade occupies an almost entirely discrete area along PC1-2 (Figure 1).	Supported. Phloeomyini occupies a unique size class, likely due to energetic constraints imposed by Chrotomyine diet, which indirectly supports a role of incumbency effects (Figure 2).
Both incumbents and secondary colonists exhibit decelerating evolutionary rates due to declining ecological opportunity	Not supported. Constant-rate diversification was a better fit for both clades (Rowsey et al. 2018 Figure 5).	Not supported. Constant-rate evolution best described Phloeomyini, decelerating rate best described Chrotomyini *but* only due to outlier morphology of *Rhynchomys*.	Not supported. Constant-rate evolution best described Phloeomyini, decelerating rate best described Chrotomyini, which is likely due to dispersal-mediated speciation, rather than ecological speciation.
Secondary clades can shift to new evolutionary modes	Not supported. Constant-rate diversification comparable to their sister clade, the Sahul old endemics, was the best fit for Chrotomyini (Rowsey et al. 2018 Figure 5).	Supported. *Rhynchomys* represents a rapid shift to a highly divergent mandibular morphology with strong support (Figure 2A)	Not supported. We recovered evidence for three shifts in mode of size evolution with varying levels of support, but only in Phloeomyini.
Secondary-colonizing clades exhibit more intraclade convergent evolution than incumbent clades	Not applicable	Not supported. The two clades have similar levels of convergence (Figure 4A).	Not supported. The two clades have similar levels of convergence (Figure 4B).
Secondary-colonizing clades exhibit lower evolutionary rates than incumbent clades	Not supported. Incumbent Phloeomyini has a lower diversification rate than Chrotomyini (Rowsey et al. 2018 Figure 6A).	Not supported. The two clades have similar rates (Figure 5A).	Strongly supported. Phloeomyini has size evolutionary rate over threefold that of Chrotomyini (Figure 5B).

for clades to evolve novel morphologies, merely that this morphological variation may be forced to be distinct from that shown by incumbent species. Although species within Chrotomyini are clustered in genera that exhibit disparate mandibular morphology from one another, field studies suggest that many of these species have similar diets (i.e., earthworms and soft-bodied arthropods; Rickart et al. 2011; Rickart et al. 2016; Heaney et al. 2016b). We suspect that focused dietary analyses may reveal differences in prey preference among chrotomyine genera (e.g., earthworms versus arthropods). If detailed dietary analyses determine that most earthworm mouse species exhibit very similar diets regardless of mandibular morphology, our PCA would suggest that the disparity in mandibular morphology reflects different prey capture strategies or habitat use facilitated by cranial morphology (e.g., fossoriality in *Chrotomys*: Zuri et al. 1999).

The diversity of chrotomyine mandibular morphology compared with their apparent lack of size and dietary diversity contrasts with Phloeomyini, which appear to be evolving disparate sizes coincident with distinct diet types (e.g., large folivores such as *Phloeomys* and small granivores such as *Musseromys*).

Bioenergetic demands may favor an increased body size in folivores such as *Phloeomys* and *Crateromys* due to availability of slow-releasing nutrients in leaves. The primarily insectivorous and vermivorous chrotomyines may be constrained to small and medium body sizes due to the accessibility of high-nutrient prey items at smaller sizes and the infeasible absolute amount of prey biomass needed for subsistence on these diet types as body size increases (Demment and Van Soest 1985; Gittleman 1985; Churchfield 1990, Churchfield 2002). This bioenergetic constraint, along with the observation that all the large-bodied phloeomyines possess some climbing ability, suggests that evolution of increased size is most likely to favor arboreal, folivorous species that occur in habitats with dense canopy foliage. Evolving a larger body size can thus permit access to a more abundant food source than available to vermivores and insectivores (Millar and Hickling 1990). If the observed lack of morphospace overlap is due to diet-related, constrained body size evolution in Chrotomyini, the fourfold lower rates of size evolution and large size class exclusion in this clade would be consistent with phloeomyine incumbency limiting ecological opportunity. However, because body size is correlated with many aspects of organismal behavior and physiology, there are multiple interpretations for the partial lack of overlap we observed. Thus, rather than phloeomyine competition preventing evolution into this large size class, the resultant size distributions may simply be the result of independent radiations due to different evolutionary pathways of least genetic resistance with little influence of interclade competition (Schluter 1996). As a result, we cannot definitively link size diversity with interspecific competitive partitioning of habitat and food resources between the two clades.

Our recovery of decelerating body size evolution in Chrotomyini in the face of constant lineage diversification is likely due to a mixture of early ecological diversification followed by dispersal-mediated speciation in this clade. Early diversification of chrotomyines on Luzon appears to have been accompanied by relatively rapid size evolution, corresponding to genus-level differences in current species diversity (Fig. 3B). Paleogeological land-area estimates of Luzon suggest the beginning period of intrageneric divergence among Chrotomyines, approximately 3–5 million years ago, was a time of rapid volcanic activity and therefore of both island and mountain building (Hall 2013). This dynamism may have created new habitat that allowed for a shift from ecological size evolution to dispersal-mediated speciation with limited body size evolution (e.g., Justiniano et al. 2015). By contrast, we suspect our lack of support for decelerating evolution in Phloeomyini may stem from lack of intraisland speciation within genera in this clade. For example, although many species in the chrotomyine genus *Apomys* appear to have diverged due to intraisland dispersal and subsequent isolation (Justiniano et al. 2015), several members of Phloeomyini have not dispersed from the oldest region of Luzon, the Central Cordillera (e.g., *Carpomys, Crateromys*) or appear to have maintained population connectivity across areas that present gene flow barriers to chrotomyine species (*Phloeomys*), resulting in lower species diversity and less power to detect decelerating body size evolution.

Rowsey et al. (2018) recovered a significantly lower diversification rate in Phloeomyini than Chrotomyini despite Phloeomyini's incumbent status. In conjunction with our findings that Phloeomyini not only exhibits a constant rate of size evolution (Table 2) but also that this evolutionary rate is much higher than that of Chrotomyini (Fig. 5B), we suspect that future work examining the relationship between body size evolution and lineage diversification across a broader sample of murines may find that increased body size may promote dispersal ability and inhibit lineage diversification (Claramunt et al. 2012; Weeks and Claramunt 2014). If this is indeed the case, an inverse relationship between rates of body size evolution and lineage diversification would explain the patterns we recovered better than resulting from incumbency effects and ecological opportunity in the absence of dispersal to other mountains on Luzon.

Previous work among muroid rodents corroborates our results of tempo and mode of mandibular evolution. Alhajeri et al. (2016) tested whether muroid rodents exhibited EB evolution consistent with declining ecological opportunity following continental colonization in a suite of ecologically important morphological characters. From a different perspective, Rowe et al. (2016) documented the remarkable convergence among independently evolving carnivorous rodents that exhibit shrewlike morphology (such as *Soricomys* and *Archboldomys* on Luzon, and *Melasmothrix* on Sulawesi) as well as the bizarre "tweezer-snouted" morphology exhibited by *Rhynchomys* on Luzon and *Paucidentomys* on Sulawesi (Rowe et al. 2016). Both Alhajeri et al. (2016) and Rowe et al. (2016) came to similar conclusions as we did: the classical model of early-burst evolution used to support a hypothesis of adaptive radiation is not the likely mechanism of morphological evolution in muroids broadly, murines specifically, nor even LOE rodents locally. Instead, a constant background process with some major shifts to new adaptive zones appears to provide a better explanation of the observed morphological variation, with similar selective pressures in convergently evolved carnivorous rodents (Table 1, Fig. 2, Table S4).

In response to the growing interest in detecting EBs in the macroevolutionary history of diverse clades, Moen and Morlon (2014) emphasized two important points for analyzing phenotypic data in the context of ecological opportunity and adaptive radiation, which Alhajeri et al. (2016) noted as potential reasons for not recovering a signal of EB morphological evolution. First, the time scale on which adaptive radiation often occurs is typically only detectable in recent radiations, such as Darwin's finches (Sato et al. 2001) and the African lake cichlids of Malawi

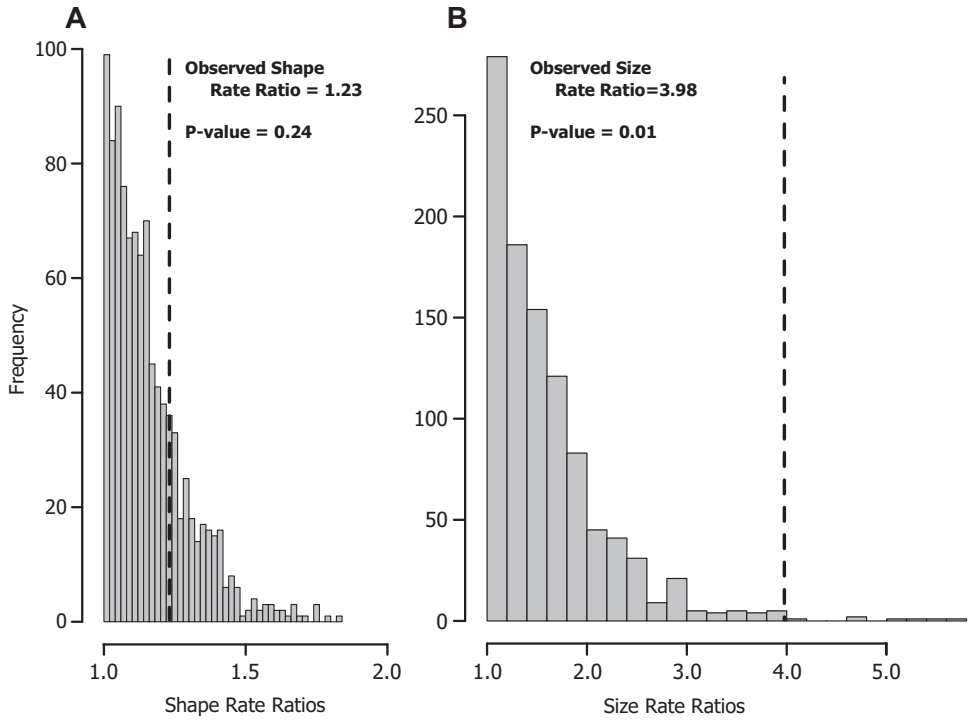

Figure 5. Histograms of simulated cladewise evolutionary rate ratios for multivariate shape data (A) and log-transformed centroid size (B). Bars represent bins of 999 calculated ratios simulated under a single-rate Brownian motion process. Dashed line indicates the observed ratio of evolutionary rates of Phloeomyini to Chrotomyini.

and Victoria (Friedman et al. 2013), with the potential for other processes to obscure this signal at longer time scales, including the scale of LOE evolution. Second, analysis of phenotypic data may be more robust to unsampled extinct taxa in detecting the historical signature of ecological opportunity, compared to analyses of lineage diversification, due to predictable patterns of trait variation among species in constant-rate versus decelerating evolutionary processes (Moen and Morlon 2014). Nevertheless, we can hypothesize a scenario where ecologically similar incumbent lineages may have selectively been driven extinct by subsequent colonists that, through mechanisms such as increased reproductive rate or foraging efficiency by secondary colonists, may have been able to overcome the incumbency effect (i.e., a competition-mediated taxon cycle: Ricklefs and Bermingham 2002). In the absence of fossil data, however, we cannot currently test this hypothesis, and the low extinction rate in Phloeomyini reported by Rowsey et al. (2018) provides some evidence to suggest that this scenario may be unlikely.

Our study is focused on the morphological evolution in the two oldest most species-rich clades on Luzon, which account for the majority of non-volant mammalian species and morphological diversity in this system. Nevertheless, an estimated four additional murine colonization events have occurred on Luzon after colonization by the LOE rodents, likely within the past 2 million years (in other words, likely long after most of the ecological differentiation corresponding to genus-level diversification had already occurred; Rowsey et al. 2018). These "new endemic" lineages are ecologically and phylogenetically distinct from the other clades, and available distributional data suggest that these rodents occur primarily in disturbed habitat types where the LOE rodents typically do not occur or are uncommon (Heaney et al. 2016b; Rowsey et al. 2018). Although these clades lack species diversity necessary for comparing tempo and mode of morphological evolution, the patterns of morphospace occupancy may suggest that the exclusion from habitat types occupied by most LOE rodents (i.e., old growth montane forest) is the result of ecological similarity to existing colonists.

Another important piece of the puzzle of incumbency effects among Indo-Australian rodents is the phylogenetic background within which Chrotomyini belongs. Chrotomyini is sister to the Sahul old endemics, so named for their range encompassing New Guinea, Australia, and Melanesian islands (SOE: Rowe et al. 2008). The incumbent status of the SOE on Sahul may approximate the potential morphological evolution realizable by Chrotomyini in the absence of an incumbent murine clade, given that Phloeomyini is endemic to the Philippines. Interestingly, several SOE genera resemble some members of the two LOE clades, including giant herbivores such as *Hyomys* and shrew-like insectivores such as *Pseudohydromys*. Analysis of phenotypic variation in these clades in a comparative evolutionary framework may

reveal the relative importance of ecological character displacement, biotic filtering, and phylogenetic inertia (Schluter 2000b). In other words, such an analysis may tell us whether the pattern of extant morphological diversity and diet type among chrotomyines is due to intrinsic (i.e., plesiomorphic) or extrinsic (i.e., incumbency-mediated) canalization of morphological evolution. Additionally, a comparison of the dietary evolution between these clades may provide evidence to suggest that the clade-specific partitioning of LOE mandibular morphology is the result of ecological and evolutionary processes to minimize potential competitive effects.

CONCLUSIONS

Our analyses of mandibular shape and size evolution illustrate several important conclusions (Table 4). First, incumbency effects may manifest both as preventative barriers to colonization by ecologically similar species as well as decreased rates of evolution in secondary colonists, but both patterns need not occur in systems with repeated colonization. Second, decelerating phenotypic evolutionary rates are not a guaranteed consequence of incumbency effects; the ecological opportunity model may be a poor fit for dynamic island systems even if these systems (such as Luzon) are relatively small and isolated. Instead, clades may be able to explore new and innovative areas of morphospace yielding unique morphologies as long as these morphologies remain disparate from existing species. Finally, our results illustrate that the tempo and mode of morphological evolution has differed in some respects from that of lineage diversification: morphospace partitioning and size variation were consistent with incumbency effects, whereas lineage diversification was not (Rowsey et al. 2018). The strength of a macroevolutionary incumbency effect may be as little as requiring differentiation along an ecologically important trait axis; our results suggest that if this requirement is met, two clades may co-occur with relatively little impact on phenotypic or lineage evolutionary rates. Our work in this system contributes to a growing body of research suggesting that species diversity does not always approximate ecological diversity, at a variety of spatiotemporal scales, even when phylogenetic signal is present in the traits being examined (Rowe et al. 2011; Ruta et al. 2013; Mazel et al. 2017; Múrria et al. 2017), and that examining species and morphological diversity may yield different and equally informative insights (Jablonski 2008).

AUTHOR CONTRIBUTIONS

DMR, LRH, and SAJ designed the research; DMR collected and analyzed the data; and DMR, LRH, and SAJ wrote the manuscript.

ACKNOWLEDGMENTS

We would like to thank the staff of the collections housing the specimens used in this study: N. Duncan, N. Simmons, R. Voss, and E. Westwig (AMNH); A. Ferguson, J. Phelps, and the late W. Stanley (FMNH); J. Chupasko (MCZ); and D. Lunde (USNM). F.K Barker, D. Fox, and K. McNulty provided comments on drafts of the manuscript. Travel expenses and equipment purchases were made possible by a Bell Museum of Natural History Dayton Wilkie Research Award and an American Society of Mammalogists Grant-in-Aid of Research awarded to DMR. DMR was also supported by the Wallace and Mary Dayton Fellowship and a Simons Fellowship awarded by the Bell Museum of Natural History. Field research that produced most of the specimens collected by LRH and deposited at FMNH has been supported by the Barbara Brown Fund for Mammal Research of the Field Museum and the Negaunee Foundation. Field research permits were provided by the Biodiversity Management Bureau of the Philippine Department of Environment and Natural Resources.

DATA ARCHIVING

R code and digitized landmark coordinates can be found in the Dryad Digital Repository package.

The doi for our data is https://doi.org/10.5061/dryad.gb7k5d1.

LITERATURE CITED

Adams, D. C. 2014. Quantifying and comparing phylogenetic evolutionary rates for shape and other high-dimensional phenotypic data. Sys. Biol. 63:166–177.

Adams, D. C., and E. Otárola-Castillo. 2013. Geomorph: an R package for the collection and analysis of geometric morphometric shape data. Meth. Ecol. Evol. 4:393–399.

Akaike, H. 1974. A new look at the statistical model identification. IEEE Trans. Auto. Cont. 19:716–723.

Alhajeri, B. H., J. J. Schenk, and S. J. Steppan. 2016. Ecomorphological diversification following continental colonization in muroid rodents (Rodentia: Muroidea). Biol. J. Linn. Soc. 117:463–481.

Almany, G. R. 2004. Priority effects in coral reef fish communities of the Great Barrier Reef. Ecology 85:2872–2880.

Alroy, J. 1996. Constant extinction, constrained diversification, and uncoordinated stasis in North American mammals. Palaeogeo. Palaeoclim. Palaeoecol. 127:285–311.

Bambach, R. K., A. H. Knoll, and J. J. Sepkoski, Jr. 2002. Anatomical and ecological constraints on Phanerozoic animal diversity in the marine realm. Proc. Nat. Acad. Sci. USA 99:6854–6859.

Betancur-R. R., G. Ortí, A. M. Stein, A. P. Marceniuk, and R. A. Pyron. 2012. Apparent signal of competition limiting diversification after ecological transitions from marine to freshwater habitats. Ecol. Lett. 15:822–830.

Bolnick, D. I. 2004. Can intraspecific competition drive disruptive selection? An experimental test in natural populations of sticklebacks. Evolution 58:608–618.

Blomberg, S. P., T. Garland, and A. R. Ives. 2003. Testing for phylogenetic signal in comparative data: behavioral traits are more labile. Evolution 57:717–745.

Burbrink, F. T., and R. A. Pyron. 2010. How does ecological opportunity influence rates of speciation, extinction and morphological diversification in New World ratsnakes (tribe Lampropeltini)? Evolution 64:934–943.

Churchfield, S. 1990. The natural history of shrews. Cornell Univ. Press, Ithaca, NY.

Churchfield, S. 2002. Why are shrews so small? The costs and benefits of small size in northern temperate *Sorex* species in the context of foraging habits and prey supply. Acta Theriol. 47:169–184.

Claramunt, S., E. P. Derryberry, J. V. Remsen Jr., and R. T. Brumfield. 2012. High dispersal ability inhibits speciation in a continental radiation of passerine birds. Proc. R. Soc. B. 279:1567–1574.

Clavel, J., G. Escarguel, and G. Merceron. 2015. mvMORPH: an R package for fitting multivariate evolutionary models to morphometric data. Meth. Ecol. Evol. 6:1311–1319.

Demment, M. W., and P. J. Van Soest. 1985. A nutritional explanation for body-size patterns of ruminant and nonruminant herbivores. Am. Nat. 125:641–672.

Derryberry, E. P., S. Claramunt, G. Derryberry, R. T. Chesser, J. Cracraft, A. Aleixo, J. Pérez-Emán, J. V. Remsen, Jr., and R. T. Brumfield. 2011. Lineage diversification and morphological evolution in a large-scale continental radiation: the neotropical ovenbirds and woodcreepers (Aves: Furnariidae). Evolution 65:2973–2986.

Duchen, P., C. Leuenberger, S. M. Szilágy, L. Harmon, J. Eastman, M. Schweizer, and D. Wegmann. 2017. Inference of evolutionary jumps in large phylogenies using Lévy processes. Syst. Biol. 66:950–963.

Emerson, B. C. 2002. Evolution on oceanic islands: molecular phylogenetic approaches to understanding pattern and process. Mol. Ecol. 11:951–986.

Emerson, B. C., and R. G. Gillespie. 2008. Phylogenetic analysis of community assembly and structure over space and time. Trend. Ecol. Evol. 23:619–630.

Engel, S. R., K. M. Hogan, J. F. Taylor, and S. K. Davis. 1998. Molecular systematics and paleobiogeography of the South American sigmodontine rodents. Mol. Biol. Evol. 15:35–49.

Felsenstein, J. 1985. Phylogenies and the comparative method. Am. Nat. 125: 1–15.

Filardi, C. E., and R. G. Moyle. 2005. Single origin of a pan-Pacific bird group and upstream colonization of Australasia. Nature 438:216–219.

Friedman, M., B. P. Keck, A. Dornburg, R. I. Eytan, C. H. Martin, C. D. Hulsey, P. C. Wainwright, and T. J. Near. 2013. Molecular and fossil evidence place the origin of cichlid fishes long after Gondwanan rifting. Proc. Biol. Sci. 280. https://doi.org/10.1098/rspb.2013.1733

Fukami, T. 2004. Assembly history interacts with ecosystem size to influence species diversity. Ecology 85:3234–3242.

Gillespie, R. G. 2004. Community assembly through adaptive radiation in Hawaiian spiders. Science 303:356–359.

Gittleman, J. L. 1985. Carnivore body size: ecological and taxonomic correlates. Oecologia 67:540–554.

Givnish, T. J., K. C. Millam, A. R. Mast, T. B. Paterson, T. J. Theim, A. L. Hipp, J. M. Henss, J. F. Smith, K. R. Wood, and K. J. Sytsma. 2009. Origin, adaptive radiation and diversification of the Hawaiian lobeliads (Asterales: Campanulaceae). Proc. Roy. Soc. B. 276:407–416.

Goldberg, E. E., and R. Lande. 2007. Species' borders and dispersal barriers. Am. Nat. 170:297–304.

Gower, J. C. 1975. Generalized Procrustes analysis. Pscyhometrika 40: 33–51.

Grossnickle, D. M., and P. D. Polly. 2013. Mammal disparity decreases during the Cretaceous angiosperm radiation. Proc. Roy. Soc. B. 280:1–8.

Gunz, P., P. Mitteroecker, S. Neubauer, G. W. Weber, and F. L. Bookstein. 2009. Principles for the virtual reconstruction of hominin crania. J. Hum. Evol. 57:48–62.

Hall, R. 2013. The palaeogeography of Sundaland and Wallacea since the Late Jurassic. J. Limno. 72:1–17.

Harmon, L. J., J. A. Schulte II, A. Larson, and J. B. Losos. 2003. Tempo and mode of evolutionary radiation in iguanian lizards. Science 301:961–964.

Harmon, L. J., J. T. Weir, C. D. Brock, R. E. Glor, and W. Challenger. 2008. GEIGER: investigating evolutionary radiations. Bioinformatics 24:129–131.

Harmon, L. J., J. B. Losos, T. J. Davies, R. G. Gillespie, J. L. Gittleman, W. B. Jennings, K. H. Kozak, M. A. McPeek, F. Moreno-Roark, T. J. Near, et al. 2010. Early bursts of body size and shape evolution are rare in comparative data. Evolution 64:2385–2396.

Hautier, L. R. Lebrun, S. Saksiri, J. Michaux, M. Vianey-Liaud, et al. 2011. Hystricognathy *vs* sciurognathy in the rodent jaw: a new morphometric assessment of hystricognathy applied to the living fossil *Laonastes* (Diatomyidae). PLoS ONE 6:1–11.

Heaney, L. R., D. S. Balete, M. R. M. Duya, M. V. Duya, S. A. Jansa, S. J. Steppan, and E. A. Rickart. 2016a. Doubling diversity: a cautionary tale of previously unsuspected mammalian diversity on a tropical oceanic island. Front. Biogeogr. 8:1–19.

Heaney, L. R., D. S. Balete, and E. A. Rickart. 2016b. The mammals of Luzon island: biogeography and natural history of a Philippine fauna. Johns Hopkins Univ. Press, Baltimore, MD.

Hurvich, C. M., and C.-L. Tsai. 1989. Regression and time series model selection in small samples. Biometrika. 76:297–307.

Jablonski, D. 2008. Biotic interactions and macroevolution: extensions and mismatches across scales and levels. Evolution 62:715–739.

Jablonski, D., and J. J. Sepkoski, Jr. 1996. Paleobiology, community ecology, and scales of ecological pattern. Ecology 77:1367–1378.

Jansa, S. A., F. K. Barker, and L. R. Heaney. 2006. The pattern and timing of diversification of Philippine endemic rodents: evidence from mitochondrial and nuclear gene sequences. Syst. Biol. 55:73–88.

Jønsson K. A., J. Lessard, and R. E. Ricklefs. 2015. The evolution of morphological diversity in continental assemblages of passerine birds. Evolution 69:879–889.

Justiniano, R., J. J. Schenk, D. S. Balete, E. A. Rickart, J. A. Esselstyn, L. R. Heaney, and S. J. Steppan. 2015. Testing diversification models of endemic Philippine forest mice (*Apomys*) with nuclear phylogenies across elevational gradients reveals repeated colonization of isolated mountain ranges. J. Biogeogr. 42:51–64.

Klingenberg, C. P., and W. Ekau. 1996. A combined morphometric and phylogenetic analysis of an ecomorphological trend: pelagization in Antarctic fishes (Perciformes: Nototheniidae). Biol. J. Linn. Soc. 59:143–177.

Landis, M. J., J. G. Schraiber, and M. Liang. 2013. Phylogenetic analysis using Lévy processes: finding jumps in the evolution of continuous traits. Syst. Biol. 62:193–204.

Lecompte, E., K. Aplin, C. Denys, F. Catzeflis, M. Chades, and P. Chevret. 2008. Phylogeny and biogeography of African Murinae based on mitochondrial and nuclear gene sequences, with a new tribal classification of the subfamily. BMC Evol. Biol. 8:1–21.

Louette, G., and L. De Meester. 2007. Predation and priority effects in experimental zooplankton communities. Oikos 116:419–426.

Maestri, R., B. D. Patterson, R. Fornel, L. R. Monteiro, and T. R. O. de Freitas. 2016. Diet, bite force and skull morphology in the generalist rodent morphotype. J. Evol. Biol. 29:2191–2204.

Mahler, D. L., L. J. Revell, R. E. Glor, and J. B. Losos. 2010. Ecological opportunity and the rate of morphological evolution in the diversification of Greater Antillean anoles. Evolution 64:2731–2745.

Mazel, F., A. Ø. Mooers, G. V. Dalla Riva, and M. W. Pennell. 2017. Conserving phylogenetic diversity can be a poor strategy for conserving functional diversity. Syst. Biol. 66:1019–1027.

Millar, J. S., and G. J. Hickling. 1990. Fasting endurance and the evolution of mammalian body size. Fun. Ecol. 4:5–12.

Moen, D., and H. Morlon. 2014. From dinosaurs to modern bird diversity: extending the time scale of adaptive radiation. PLoS Biol. 12:12–15.

Múrria, C., S. Dolédec, A. Papadopoulou, A. P. Vogler, and N. Bonada. 2017. Ecological constraints from incumbent clades drive trait evolution across the tree-of-life of freshwater macroinvertebrates. Ecography 40: 1–13.

Pagel, M. 1999. Inferring the historical patterns of biological evolution. Nature 401:877–884.

Paradis, E., J. Claude, and K. Strimmer. 2004. APE: analyses of phylogenetics and evolution in R language. Bioinformatics 20:289–290.

Parent, C. E., and B. J. Crespi. 2009. Ecological opportunity in adaptive radiation of Galápagos endemic land snails. Am. Nat. 174:898–905.

Pennell, M. W., R. G. FitzJohn, W. K. Cornwell, and L. J. Harmon. 2015. Model adequacy and the macroevolution of angiosperm functional traits. Am. Nat. 186:E33–E50.

Polly, P. D., A. M. Lawing, A.-C. Fabre, and A. Goswami. 2013. Phylogenetic principal components analysis and geometric morphometrics. Hystrix It. J. Mamm. 24:33–41.

R Core Team. 2015. R: A language and environment for statistical computing. R Foundation for Statistical Computing, Vienna, Austria.

Revell, L. J. 2009. Size-correction and principal components for interspecific comparative studies. Evolution. 63:3258–3268.

Revell, L. J. 2012. Phytools: an R package for phylogenetic comparative biology (and other things). Methods Ecol. Evol. 3:217–223.

Revell, L. J., and D. C. Collar. 2009. Phylogenetic analysis of the evolutionary correlation using likelihood. Evolution 63:1090–1100.

Ribas, C. C., R. G. Moyle, C. Y. Miyaki, and J. Cracraft. 2007. The assembly of montane biotas: linking Andean tectonics and climatic oscillations to independent regimes of diversification in *Pionus* parrots. Proc. Roy. Soc. B. 274:2399–2408.

Rickart, E. A., L. R. Heaney, D. S. Balete, and B. R. Tabaranza, Jr. 2011. Small mammal diversity along an elevational gradient in northern Luzon, Philippines. Mamm. Biol. 76:12–21.

Rickart, E. A., D. S. Balete, P. A. Alviola, M. J. Veluz, and L. R. Heaney. 2016. The mammals of Mt. Amuyao: a richly endemic fauna in the Central Cordillera of northern Luzon Island, Philippines. Mammalia 80:579–592.

Ricklefs, R. E., and E. Bermingham. 2002. The concept of the taxon cycle in biogeography. Glob. Ecol. Biogeogr. 11:353–361.

Rohlf, F. J., and D. E. Slice. 1990. Extensions of the Procrustes method for the optimal superimposition of landmarks. Syst. Zool. 39:40–59.

Rowe, K. C., M. L. Reno, D. M. Richmond, R. M. Adkins, and S. J. Steppan. 2008. Pliocene colonization and adaptive radiations in Australia and New Guinea (Sahul): multilocus systematics of the old endemic rodents (Muroidea: Murinae). Mol. Phylo. Evol. 47:84–101.

Rowe, K. C., K. P. Aplin, P. R. Baverstock, and C. Moritz. 2011. Recent and rapid speciation with limited morphological disparity in the genus *Rattus*. Syst. Biol. 60:188–203.

Rowe, K. C., A. S. Achmadi, and J. A. Esselstyn. 2016. Repeated evolution of carnivory among Indo-Australian rodents. Evolution 70:653–665.

Rowsey, D. M., L. R. Heaney, and S. A. Jansa. 2018. Diversification rates of the "old endemic" murine rodents of Luzon Island, Philippines are inconsistent with incumbency and ecological opportunity. Evolution 72:1420–1435.

Ruta, M., K. D. Angielczyk, J. Fröbisch, and M. J. Benton. 2013. Decoupling of morphological disparity and taxic diversity during the adaptive radiation of anomodont therapsids. Proc. Biol. Sci. 280. https://doi.org/10.1098/rspb.2013.1071

Sato, A., C. O'Huigin, H. Tichy, P. R. Grant, B. R. Grant, and J. Klein. 2001. On the origin of Darwin's finches. Mol. Biol. Evol. 18:299–311.

Schenk, J. J., K. C. Rowe, and S. J. Steppan. 2013. Ecological opportunity and incumbency in the diversification of repeated continental colonizations by Muroid rodents. Sys. Bio. 62:837–864.

Schluter, D. 1996. Adaptive radiation along genetic lines of least resistance. Evolution 50:1766–1774.

———. 2000a. The ecology of adaptive radiation.Oxford Univ. Press, New York, NY.

———. 2000b. Ecological character displacement in adaptive radiation. Am. Nat. 156:S4–S16.

Sidlauskas, B. 2008. Continuous and arrested morphological diversification in sister clades of characiform fishes: a phylomorphospace approach. Evolution 62:3135–3156.

Simpson, G. G. 1953. The major features of evolution. New York: Columbia University Press.

Tobias, J. A., C. K. Cornwallis, E. P. Derryberry, S. Claramunt, R. T. Brumfield, and N. Seddon. 2014. Species coexistence and the dynamics of phenotypic evolution in adaptive radiation. Nature 506:359–363.

Uyeda, J. C., D. S. Caetano, and M. W. Pennell. 2015. Comparative analysis of principal components can be misleading. Syst. Biol. 64:677–689.

Verde Arregoitia, L. D., D. O. Fisher, and M. Schweizer. 2017. Morphology captures diet and locomotor types in rodents. R. Soc. Open Sci. 4:1–14.

Wainwright, P. C., W. L. Smith, S. A. Price, K. L. Tang, J. S. Sparks, L. A. Ferry, K. L. Kuhn, R. I. Eytan, and T. J. Near. 2012. The evolution of pharyngognathy: a phylogenetic and functional appraisal of the pharyngeal jaw key innovation in Labroid fishes and beyond. Syst. Biol. 61:1001–1027.

Webb, S. D. 1985. Late Cenozoic mammal dispersals between the Americas. Pp. 357–386 *in* F. G. Stehli and S. D. Webb, eds. The Great American biotic interchange. Plenum Press, New York, NY.

Weeks, B. C., and S. Claramunt. 2014. Dispersal has inhibited avian diversification in Australasian archipelagoes. Proc. R. Soc. B. 281:1–7.

Zuri, I., I. Kaffe, D. Dayan, and J. Terkel. 1999. Incisor adaptation to fossorial life in the blind mole-rat, *Spalax ehrenbergi*. J. Mamm. 80:734–741.

Associate Editor: A. Goswami
Handling Editor: Mohamed. A. F. Noor

Supporting Information

Additional supporting information may be found online in the Supporting Information section at the end of the article.

Table S1. Table of specimens and associated metadata used in this study.

Table S2. Summary of principal component analysis, including explained proportion of variance and loading matrix for all components.

Table S3. Results of univariate morphological evolutionary rate model adequacy test for standard cladewise principal component scores.

Table S4. Average model support for 100 simulated character histories of Brownian motion morphological evolution of PCs 1 and 2.

Table S5. Average model support for 100 simulated character histories of Brownian motion morphological evolution of centroid size.

Table S6. Likelihood ratio tests (LRT) of decelerating morphological evolution fitted to phylogenetically transformed PC1–2 of mandibular shape.

Table S7. Results of univariate morphological evolutionary rate model adequacy test for phylogenetically corrected cladewise component scores.

Table S8. Average model support for 100 simulated character histories of Brownian motion morphological evolution of phylogenetically corrected PC 1–2.

Figure S1. Phylomorphospace of phylogenetically-corrected principal components 1–2 for Luzon old endemic rodents.

Figure S2. Histogram of differences in cladewise covariances between Euclidean and patristic distances as a comparison of convergence between clades. The dashed line indicates the observed difference in covariances between Phloeomyini and Chrotomyini, and the gray bars represent differences simulated under a clade-independent Brownian Motion process. The Euclidean distances measured in this figure were calculated from phylogenetically-corrected PC1-5 scores.

Figure S3. Figure 1. PC1 and PC2 of mandibular morphology for 41 Luzon old endemic rodent species ($n = 337$). Specimens are colored according to their placement by genus. Thin-plate splines along axes show specimens with extreme scores and illustrate differences along these axes. Bottom-left: lateral view of mandible indicating landmarks taken. Landmarks taken are as follows: 1. Anterodorsal apex of incisive alveolus; 2. Ventral nadir of diastema between incisor (I1) and first molar (M1); 3. Anterior margin of M1 alveolus; 4. Junction of coronoid process with body of mandible, defined by point at which a straight line following coronoid process first meets the body; 5. Posterodorsal apex of coronoid process; 6. Ventral nadir between coronoid and condyloid processes; 7. Anterodorsal apex of condyloid process; 8. Posterior apex of condyloid process; 9. Anterior nadir between condyloid and angular processes; 10. Posterior apex of angular process; 11. Ventral apex of angular process; 12. Anteroventral apex of incisive alveolus.